Identification of a trafficking determinant localized to the Kv1 potassium channel pore

Louis N. Manganas*, Qiang Wang†, Robert H. Scannevin†, Dana E. Antonucci*, Kenneth J. Rhodes†, and James S. Trimmer*‡

*Department of Biochemistry and Cell Biology, State University of New York, Stony Brook, NY 11794; and †Neuroscience, Wyeth–Ayerst Research, Princeton, NJ 08543

Edited by Lily Y. Jan, University of California, San Francisco, CA, and approved September 21, 2001 (received for review August 1, 2001)

The repertoire of Kv1 potassium channels expressed in presynaptic terminals of mammalian central neurons is shaped by intrinsic trafficking signals that determine surface-expression efficiencies of homomeric and heteromeric Kv1 channel complexes. Here, we show that a determinant controlling surface expression of Kv1 channels is localized to the highly conserved pore region. Point-mutation analysis revealed two residues as critical for channel trafficking, one in the extracellular ''turret'' domain and one in the region distal to the selectivity filter. Interestingly, these same residues also form the binding sites for polypeptide neurotoxins. Our findings demonstrate a previously uncharacterized function for the channel-pore domain as a regulator of channel trafficking.

Shaker or mammalian Kv1 α- and Kvβ-subunits can assemble promiscuously into functional homo- and heterotetrameric complexes, resulting in biophysically and pharmacologically distinct $\alpha_4\beta_4$ channel complexes (1–4). However, biochemical and immunohistochemical studies have demonstrated that specific Kv1 heteromeric complexes predominate in mammalian brain, and many other possible subunit combinations are not detected (5–9). Particularly noteworthy is the absence of Kv1.1 homotetramers. These observations suggest not only a functional importance for particular heteromeric channel complexes, but that cellular mechanisms exist to restrict surface expression to only those channels with appropriate subunit composition.

Mammalian Kv1 channels are assembled in the endoplasmic reticulum (ER) (10); however, the mechanisms that regulate ER export, cell-surface expression and targeting of Kv1 channels in neurons are unknown. The rate-limiting step for trafficking/expression of most membrane proteins is ER export (11), and export competence can be determined by diverse mechanisms, including folding, assembly, and specific ER retention/export signals (12). We have found that mammalian Kv1 α-subunits possess distinct trafficking and surface-expression properties when expressed in mammalian cells including cultured hippocampal neurons (13). Therefore, we constructed a number of chimeric Kv1 α-subunits between efficiently trafficked Kv1.4 and inefficiently trafficked Kv1.1 and compared their trafficking and surface-expression properties to wild-type subunits. Our results demonstrate that a Kv1 channel-trafficking regulator is localized to the highly conserved pore region. Point-mutation analyses revealed a correlation between residues responsible for trafficking and binding to polypeptide neurotoxins. These data suggest a previously uncharacterized role for the Kv1 pore as a potential quality control mediator.

Methods

Antibodies. Antibodies generated against the cytoplasmic and extracellular domains of potassium channel α-subunits have been described (10, 13–17). Anti-vimentin (monoclonal, clone no. 9) antibody was purchased from Sigma.

Transient Transfection of COS-1 Cells. Cells were transfected with mammalian expression vectors for rat Kv1.1 (RBK1) and rat Kv1.4 (RK4) Kv channel α-subunit polypeptides (18) by the calcium phosphate precipitation method (19). Cells were seeded at 10% confluence (for biochemical analysis) or 1% confluence (for immunofluorescence) and grown at 37°C in DMEM containing 10% (vol/vol) calf serum. The calcium phosphate DNA mixture was added within 24 h of seeding, when cells were approximately twice the original plating density, and left for 18–24 h. The transfection media then was removed, and after the addition of fresh media, the cells were incubated at 37°C for an additional 24 h.

Generation of Chimeric and Mutant Kv1 α-Subunit cDNAs. Chimeric Kv1 subunits were generated by fusing PCR-generated fragments of Kv1.1 and Kv1.4 rat cDNAs in the RBG4 mammalian expression vector. Kv1 point mutants were generated by Quick Change (Stratagene) PCR mutagenesis.

Sucrose Gradient Sedimentation. One-half milligram of each protein standard (apoferritin, alcohol dehydrogenase, BSA, and carbonic anhydrase; ref. 20) and 50 μl of Kv1.1 COS-1 lysate were layered on separate 5–50% sucrose gradient (volume of $\approx$2 ml in polyalomer tubes) containing TBS (pH 8.0), 5 mM EDTA, 1% (vol/vol) Triton X-100 (TX-100), 1 mM iodoacetamide, and a protease inhibitor mixture (2 μg/ml aprotinin/1 μg/ml leupeptin/2 μg/ml antipain/10 μg/ml benzamidine/0.2 mM phenylmethylsulfonyl fluoride). Samples were centrifuged for 4h at 202,059 $\times$ *g* at 4°C, and 10 (200 μl each) fractions were manually collected from the top of the gradient. Each 200 μl fraction was added to 800 μl of lysis buffer (see above) and immunoprecipitated with 1 μg/ml of affinity-purified Kv1.1C antibody for 1h at 4°C. Protein A Sepharose (30 μl) was used to immunoprecipitate antibody complexes for 30 min at 4°C. Pellets were washed three times in ice-cold lysis buffer (without BSA), and the final pellets were resuspended in sample buffer and analyzed by SDS/PAGE and immunoblotting. The blots then were incubated in substrate for enhanced chemiluminescence for 1 min and autoradiographed on preflashed (to OD_{545} = 0.15) Fuji RX film. Densitometric measurements were obtained by using a Bio-Rad Model GS-670 imaging densitometer.

Electrophysiological Recordings. Representative traces of whole-cell currents were recorded at room temperature (RT) with the standard patch-clamp whole-cell recording method. When filled with pipette solutions, the resistance of the patch pipettes was in a range of 2–4 MΩ. The cells were voltage-clamped at -80 mV and depolarized to $+40$ mV in 10 mV increments. Currents were sampled at a rate of 250 μs per point and filtered by a low-pass

This paper was submitted directly (Track II) to the PNAS office.

Abbreviations: ER, endoplasmic reticulum; RT, room temperature; PK, proteinase K; CFTR, cystic fibrosis transmembrane conductance regulator; TX-100, Triton X-100.

‡To whom reprint requests should be addressed. E-mail: james.trimmer@sunysb.edu.

The publication costs of this article were defrayed in part by page charge payment. This article must therefore be hereby marked "*advertisement*" in accordance with 18 U.S.C. §1734 solely to indicate this fact.

Table 1. Cell surface expression of Kv1 channels

Kv1 subunit	SE
Kv1.1 wild type	−
A352P	+
E353T	−
Y379K	+/−
A352P/E353T	+/−
A352P/Y379K	+/−
E353T/Y379K	−
A352P/E353T/Y379K	+/−
Kv1.4 wild type	+
P505A	+
T506E	+
K532Y	+
P505A/T506E	+
P505A/K532Y	−
T506E/K532Y	+
P505A/T506E/K532Y	−

Bessel filter set at 1 kHz. Membrane currents were both leak- and capacity-subtracted on line with a p/4 subtraction protocol.

Immunofluorescence Staining of Transfected Cells. Cells expressing rat Kv1 α-subunits were stained 48 h posttransfection with a surface immunofluorescence protocol (10, 13, 17). Cells were washed three times in ice-cold PBS (10 mM phosphate buffer, pH 7.4/0.15 M NaCl) containing 1 mM $MgCl_2$ and 1 mM $CaCl_2$ and then fixed in the same buffer containing 4% (wt/vol) paraformaldehyde for 30 min at 4°C. After three washes with PBS, nonspecific protein-binding sites were blocked with Blotto (4% nonfat dry milk powder in TBS (10 mM Tris·HCl, pH 7.5/0.15 M NaCl) for 1 h at RT and then incubated with mouse or rabbit ectodomain-directed antibodies for 1 h at RT. After washing three times with Blotto, cells were permeabilized with Blotto containing 0.1% TX-100 (Blotto + T) for 1 h at RT. This treatment was followed by incubation with cytoplasmically directed antibodies (derived from the species distinct from that used for the ectodomain staining) for 1 h at RT. Cells were washed three times in Blotto + T, incubated with Texas red goat anti-rabbit and FITC goat anti-mouse diluted in Blotto + T for 1 h and washed three times with PBS containing 0.1% TX-100. For standard immunofluorescence staining, 0.1% TX-100 was included during fixation.

Cells were viewed under indirect immunofluorescence on a Zeiss Axioskop microscope. Surface vs. total staining was scored under narrow-wavelength fluorescein and Texas red filter sets. The percentage of Kv1-expressing cells with detectable surface Kv1 staining was determined and defined as surface expression (SE). [(+) = >85%; (−) = <3%; and (+/−) = 10–50% of cells expressing Kv1 channels on the cell surface.]

Preparation of Soluble and Insoluble Fractions. Transfected COS-1 cells were permeabilized in lysis buffer containing TX-100 (13). The crude lysates were centrifuged at 4°C for 5 min at 14,000 × *g*. An equal volume of reducing SDS sample buffer (2×) was added to soluble fractions (13). Insoluble fractions were washed three times with ice-cold PBS and added to 1× reducing SDS sample buffer. Samples were boiled and fractioned on SDS/7.5% polyacrylamide gels. Gel electrophoresis and immunoblotting have been described (13). Blots were incubated in substrate for enhanced chemiluminescence for 1 min and autoradiographed on preflashed (to OD_{545} = 0.15) Fuji RX film.

Enzymatic Digestion. For Proteinase K digestion (Sigma), transfected cells were washed three times with ice-cold PBS. Each 35-mm dish was incubated with 10 mM Hepes/150 mM NaCl/2 mM $CaCl_2$ (pH 7.4) with or without 200 μg/ml Proteinase K (13, 21) at 37°C for 30 min. The cells then were harvested and centrifuged at 4°C at 1,000 × *g* in a refrigerated microcentrifuge; Proteinase K digestion was quenched by adding ice-cold PBS containing 6 mM phenylmethylsulfonyl fluoride and 25 mM EDTA. This treatment was followed by three washes in ice-cold PBS. Cleared lysates were prepared and analyzed by immunoblotting, as described above.

Primary Hippocampal Cultures. Hippocampal cultures were prepared as described (13, 22–24). Cultured hippocampal neurons at 7 days *in vitro* were transfected by the Lipofectamine Plus method (Life Technologies, Rockville, MD), as described (24).

Results

Analysis of the deduced amino acid sequences of Kv1.1 and Kv1.4 reveals a highly conserved core domain (between transmembrane segments S1 and S6) and highly variable cytoplasmic N and C termini (25). Surprisingly, our detailed chimera analysis (Fig. 1*A*) revealed that any chimera containing the Kv1.1 sequence between transmembrane segments S5 and S6 was retained in the ER, including chimera I, which is composed of 613 amino acids of Kv1.4 and 41 amino acids of Kv1.1. Moreover, any chimera containing the analogous region of Kv1.4 is efficiently expressed on the cell surface, including chimera J, containing 454 amino acids of Kv1.1 and 41 amino acids of Kv1.4. Chimera I, like Kv1.1, was localized to the ER (Fig. 1*B*), a distribution never observed for wild-type Kv1.4 (13). In contrast Kv1.4 and chimera J had plasma-membrane localization (Fig. 1*B*). When live COS-1 cells transfected with these channels were treated with PK and subsequently assayed by immunoblots, Kv1.4 and Chimera J exhibited a substantial PK-sensitive (i.e., cell-surface) population, whereas Kv1.1 and Chimera I did not (Fig. 1*C*). Forty-five percent of the total Chimera J pool was sensitive to PK digestion, similar to the PK-sensitive component of the wild-type Kv1.4 pool (54 ± 2.0%). Taken together, these immunofluorescence and biochemical data suggest that Kv1 channel trafficking is influenced by the pore region.

Recently, a previously uncharacterized cellular response to misfolded proteins was identified and termed the aggresome response (26). Aggresomes form when the intermediate filament protein vimentin sequesters misfolded protein aggregates. To determine whether misfolding was responsible for the ER retention of Kv1.1, we double-labeled transfected cells for Kv1.1 and vimentin and compared the number of cells forming aggresomes to cells expressing the cystic fibrosis transmembrane conductance regulator (CFTR) folding mutant, CFTR (ΔF508). Our results show that 5% of cells expressing Kv1.1 displayed aggresome formation, whereas 54% of the cells expressing CFTR ΔF508 formed aggresomes (Fig. 2*A*). To assess folding biochemically, Kv1.1 was expressed in COS-1 cells and analyzed for solubility in buffers containing different concentrations of the nonionic detergent TX-100, a useful indicator of the folding state of membrane proteins (27). We found that, like Kv1.4, Kv1.1 was soluble even at the lowest concentration of TX-100 (0.1%; Fig. 2*B*). These immunofluorescence and biochemical data are consistent with no obvious folding defects.

Unassembled and misassembled membrane-protein complexes are retained in the ER and degraded by quality control mechanisms. To determine whether Kv1.1 ER retention is simply due to a defect in tetramerization, membrane extracts containing Kv1.1 channels were analyzed on nondenaturing continuous sucrose-density gradients (20). We found that the bulk of the Kv1.1 protein appeared in the fraction that contains proteins of apparent molecular mass in a range of ≈165–285 kDa (Fig. 2*C*). As the estimated molecular mass of Kv1.1 tetramers

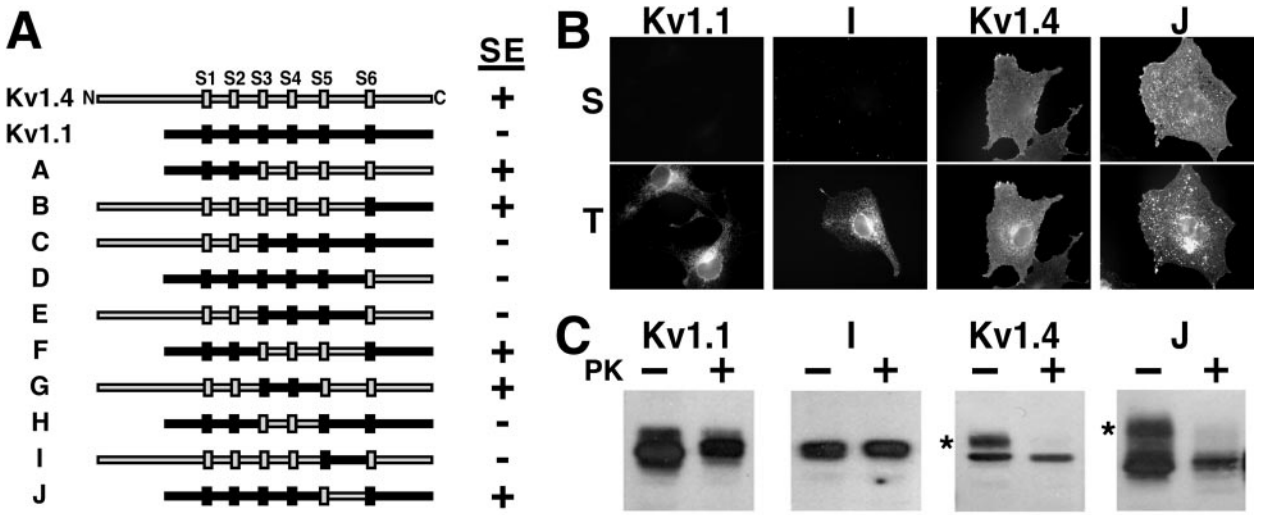

Fig. 1. The P-domain regulates trafficking of Kv1 channels. (*A*) The Kv1 chimeras generated are as follows: A, Kv1.1N(1–253)–1.4C(405–654); B, Kv1.4N(1–542)–1.1C(390–495); C, Kv1.4N(1–404)–1.1C(254–495); D, Kv1.1N(1–389)–1.4C(543–654); E, Kv1.4N(1–404)–1.1(254–389)-1.4C(543–654); F, Kv1.1N(1–253)–1.4(405–542)-1.1C(390–495); G, Kv1.4N(1–404)–1.1(254–322)-1.4C(474–654); H, Kv1.1N(1–253)–1.4(405–474)-1.1C(322–495); I, Kv1.4N(1–474)–1.1(322–389)-1.4C(543–654); J, Kv1.1N(1–321)–1.4(475–542)-1.1C(390–495). SE values for Kv1 chimeras were determined: (+) = >85%, (−) = <3%, and (+/−) = 10–50% of cells express Kv1 channels on the cell surface. Chimeras I and J define the P-domain between transmembrane segments S5 and S6 as the trafficking determinant. (*B*) Subcellular localization of wild-type and chimeric Kv1 subunits. Chimeras I and J recapitulate the subcellular localization of wild-type Kv1.1 and Kv1.4 subunits, respectively. Kv1.1 and Chimera I accumulate in the ER, whereas Kv1.4 and Chimera J are present on the cell surface. S, surface staining with an ectodomain-directed antibody in the absence of detergent permeabilization; T, total staining with a cytoplasmic domain-directed antibody after detergent permeabilization. (*C*) Biochemical analysis reveals proteinase K (PK) cell-surface populations of Kv1.4 and Chimera J (asterisks) but not Kv1.1 or Chimera I.

is 224 kDa, we can conclude that soluble pools of wild-type Kv1.1 subunits may form tetramers.

The Kv1 trafficking determinant localizes entirely to a sequence in the linker between transmembrane segments S5 and S6. This 41-aa region contains the bulk of the residues that form the channel pore (28) and, as such, is referred to as the P-domain (Fig. 3*A*). The three variable P-loop positions (shaded regions, Fig. 3*A*) were individually mutated from those in Kv1.1 to those in Kv1.4, and vice-versa. Kv1.1A352P exhibited a dramatic increase in cell-surface expression, whereas Kv1.1E353T and Kv1.1Y379K showed little or no change (Table 1). Similar results were obtained when voltage-gated K^+ currents were analyzed by whole-cell patch clamping (Fig. 3*B*). The current density in cells expressing Kv1.1A352P (688.3 ± 119.3 pA/pF, $n = 10$) was significantly ($P = 0.015$) larger than in cells expressing Kv1.1 (245.3 ± 49.6 pA/pF, $n = 6$) or E353T (189.6 ± 22.0 pA/pF, $n = 4$; $P = 0.41$ vs. wild type); no current was detected in Y379K-expressing cells. None of the reciprocal Kv1.4 single point mutants exhibited altered surface expression, although double and triple Kv1.4 point mutants containing both the P505A and K532Y mutations exhibited dramatically decreased surface expression (Table 1). Although cell-surface expression of Kv1.1A352P and Kv1.4 was similar, considerable ER pools of Kv1.1A352P were observed (Fig. 3*C*, arrow). Furthermore, the percentage of the total PK-sensitive Kv1.4 (52.0 ± 3.0%) and Kv1.1A352P (8.0 ± 1.0%) pools were also quite different, suggesting that the Kv1.1A352P mutation is not as efficiently trafficked to the cell surface as are wild-type Kv1.4 and chimera J. This finding may reflect a requirement for Kv1.4 residues within the P-loop other than those described here.

The dramatic difference in surface expression of wild-type and mutant Kv1 subunits also was observed in cultured rat hippocampal neurons, which do not express detectable levels of endogenous Kv1 subunits at the stage of culture (7–9 days *in vitro*) used for these experiments (13). Kv1.1A352P exhibited robust surface staining, whereas Kv1.4P505A/K532Y was not detected on the cell surface and was localized intracellularly (Fig. 3*D*). Thus, the P-domain amino acids can regulate Kv1 channel-surface expression in both neuronal and non-neuronal cells.

Discussion

The mechanisms that regulate surface expression of Kv1 channels in neurons remain to be elucidated. The rate-limiting step for trafficking/surface expression of most membrane proteins is ER export (11), and export competence can be determined by diverse mechanisms, including assembly, folding, ER retention/retrieval, or ER export signals found on component subunits (12). Previously, we have shown that the stoichiometry of Kv1.1 and Kv1.4 subunits within a Kv1 tetramer play a critical role in trafficking in neurons (13). Recently, variations of a cytoplasmic C-terminal ER-export motif (VxxSL) for regulating Kv1.2- and Kv1.4-channel surface expression were described (29). Our immunofluorescence and biochemical data on Kv1.1/Kv1.4 chimeras strongly suggest that the pore domain plays a dominant role in regulating the trafficking of Kv1 channels to the plasma membrane. However, our data do not eliminate the possibility that the cytoplasmic C terminus can further influence Kv1-channel trafficking. For example, the Kv1.1 pore could act as a signal responsible for ER retention of Kv1 channels. Once pore-mediated ER retention is suppressed, through heteromultimerization with Kv1.2 or Kv1.4 subunits (13), subsequent ER export could be affected by cytoplasmic C-terminal VxxSL motifs.

These trafficking determinants may act during biosynthesis as assembly and/or folding determinants (30–32). Studies on nicotinic acetylcholine receptors biosynthesis have shown ER export is controlled by ER chaperones that allow export of only properly assembled $\alpha 2\beta\gamma\delta$ receptors (33), whereas export of mutant CFTR (ΔF508) subunits is limited by misfolding (34). Our immunofluorescence and biochemical results show that like Kv1.4, Kv1.1 is soluble in nonionic detergent and does not form aggresomes, which is consistent with proper folding. However, these assays may detect only gross misfolding of membrane proteins, and it remains possible that ER retention of Kv1.1

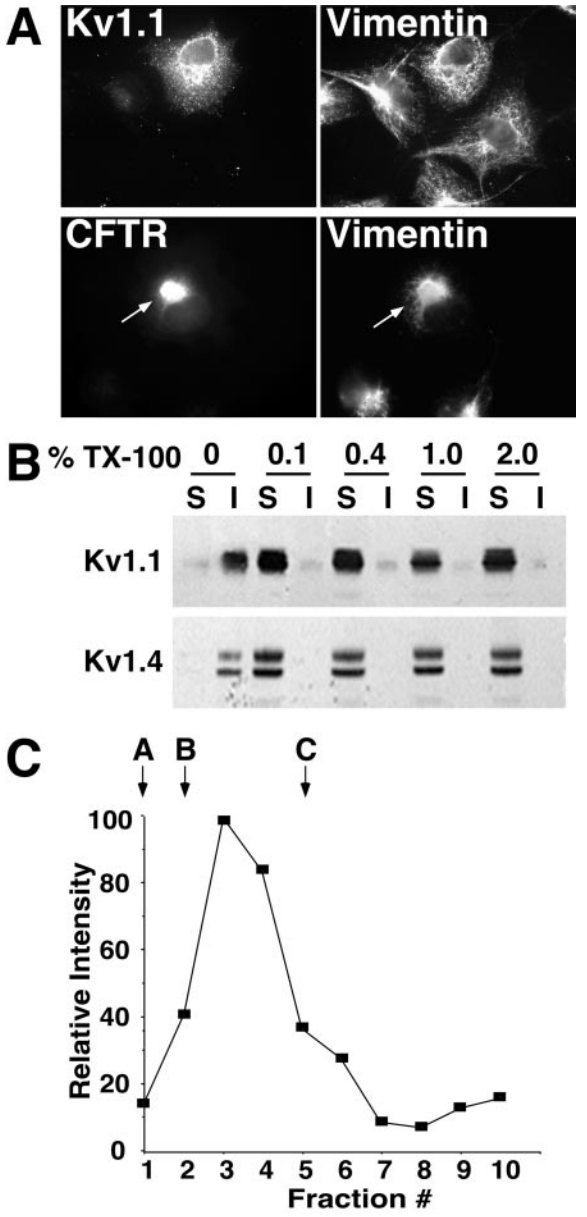

Fig. 2. Folding and assembly of Kv1 channels. *(A)* COS-1 cells expressing Kv1.1 (*Upper*) or CFTRΔF508-GFP (*Lower*) were fixed, permeabilized, and stained with anti-Kv1.1 (*Upper Left*) and anti-vimentin (*Upper and Lower, Right*). Arrows show aggresome formation, indicated by vimentin collapse into ring-like structures. *(B)* COS-1 cells expressing Kv1.1 (*Upper*) or Kv1.4 (*Lower*) were harvested and permeabilized in lysis buffer containing 0%, 0.1%, 0.4%, 1.0%, or 2.0% TX-100 detergent. Soluble (S) and insoluble (I) fractions were separated by centrifugation and analyzed by SDS/PAGE and immunoblotting. *(C)* COS-1 cells expressing Kv1.1 were harvested and permeabilized with 1.0% TX-100. Soluble lysates were fractionated on a 5–50% linear nondenaturing sucrose gradient. Fractions were subjected to immunoprecipitation, SDS/PAGE, immunoblotting, and densitometry. Gradient controls are as follows: A, carbonic anhydrase; B, BSA and alcohol dehydrogenase; and C, apoferritin.

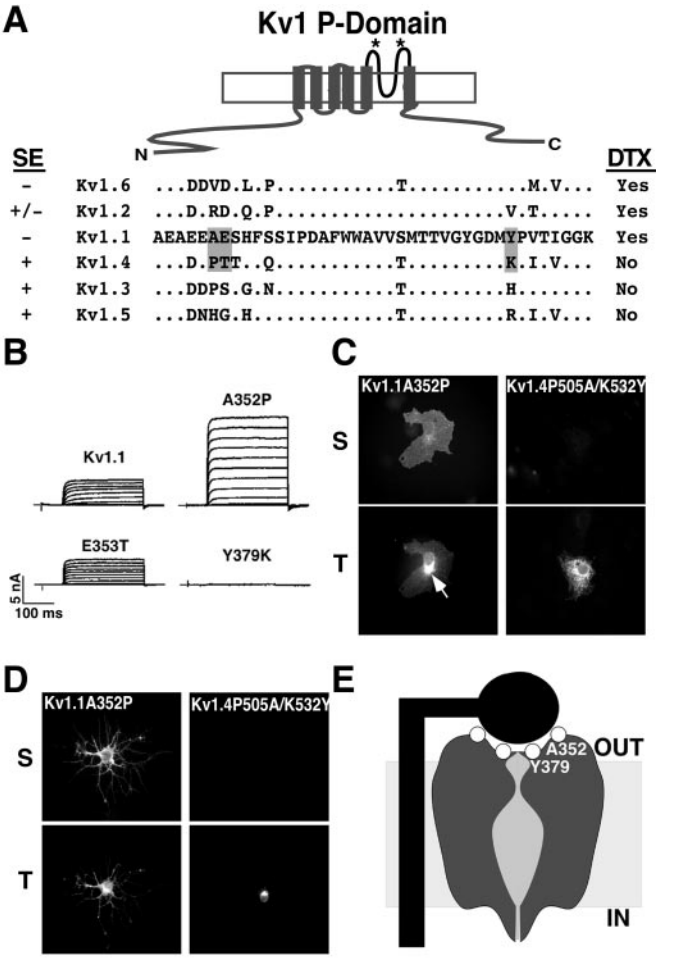

Fig. 3. Identification of P-loop residues critical for Kv1 trafficking. (*A*) Cartoon of predicted membrane topology of Kv1 subunits; the P-domain residues are colored in black. Sequence alignment of P-domain sequences of all brain Kv1 subunits. Residues within the 40-aa P-domain of Kv1 subunits are aligned and compared with the SE value. Residues identical to those in Kv1.1 are not shown. Shaded regions show the most divergent positions between ER retained (−), intermediate (+/−) and efficiently trafficked (+) Kv1 subunits. Asterisks in cartoon indicate relative positions of shaded residues within the P-Domain of the cartoon of Kv1 topology. (*B*) Kv1.1A352P yields enhanced currents compared with wild-type Kv1.1. (*C*) Subcellular localization of mutant Kv1 subunits. Kv1.1A352P-expressing cells exhibit extensive cell-surface staining but also have an intracellular pool (arrow) not detected for wild-type Kv1.4 or chimera J. Kv1.4P505A/K532Y-expressing cells exhibit ER-associated staining similar to wild-type Kv1.1. S, surface staining with an ectodomain-directed antibody in the absence of detergent permeabilization; T, total staining with a cytoplasmic domain-directed antibody after detergent permeabilization. (*D*) Mutations in P-loop residues alter surface expression in hippocampal neurons. Cultured rat hippocampal neurons were assayed for surface staining (S) and total staining (T), as described above. (*E*) Cartoon depiction of a potential interaction between an ER protein (black) and a Kv1 channel (gray). Specific pore residues thought to be involved are colored in white. OUT, ER lumen; IN, cytoplasmic space.

channels may be mediated by misfolding and interaction with ER chaperones. Our sucrose-gradient data show that Kv1.1 channels form tetramers in COS-1 cells, suggesting that ER retention is not due to complete lack of assembly of Kv1.1. However, lack of proper assembly of more restricted domains, and perhaps the pore domain itself, could contribute to the ER retention of Kv1.1. Furthermore, whether the Kv1 pore domain can efficiently multimerize with some Kv1 subunits and not others is not known.

The amino acid residues shown here to be critical for trafficking can be mapped to the crystal structure of the Kcsa channel (35); they are located in the extended extracellular turret domain (Kv1.1A352 = Kv1.4P505 = KcsaP55) or in the external mouth of the channel pore (Kv1.1Y379 = Kv1.4K532 = KcsaY82), in close proximity to one another. Interestingly, these same residues are necessary for high-affinity binding of the polypeptide neurotoxin α dendrotoxin (DTX) to Kv1.1 (36, 37). Moreover, it is intriguing that all DTX-sensitive Kv1 subunits

(Kv1.1, Kv1.2, and Kv1.6) are retained in the ER, whereas all DTX-insensitive Kv1 subunits (Kv1.3, Kv1.4, and Kv1.5) are efficiently trafficked to the cell surface (Fig. 3*A*). Together, these structural and toxin-binding results show that the trafficking determinant identified here comprises the external face of the pore and participates in high-affinity binding of polypeptide neurotoxins (35, 37, 38), such that interaction with a pore-binding ER chaperone or retention receptor is feasible (Fig. 3*E*). It is possible that such a pore-binding protein may act to block Kv1 channel conductance while in the ER, preventing alterations in ER-membrane potential and/or luminal ionic milieu during biosynthetic transit of Kv1 channels.

We thank J. Engebrecht, G. Mandel, and M. Rasband (State University of New York, Stony Brook) for critical reading of the manuscript, and R. Kopito (Stanford University) for the CFTR plasmids. This work was supported by National Institutes of Health Grant NS34383 (to J.S.T.), Wyeth-Ayerst Research, Princeton, NJ, and the Center for Biotechnology at Stony Brook, and funded by the New York State Science and Technology Foundation.

1. Isacoff, E. Y., Jan, Y. N. & Jan, L. Y. (1990) *Nature (London)* **345,** 530–534.
2. Ruppersberg, J. P., Schroter, K. H., Sakmann, B., Stocker, M., Sewing, S. & Pongs, O. (1990) *Nature (London)* **345,** 535–537.
3. Hopkins, W. F., Allen, M. L., Houamed, K. M. & Tempel, B. L. (1994) *Pflügers Arch.* **428,** 382–390.
4. Rettig, J., Heinemann, S. H., Wunder, F., Lorra, C., Parcej, D. N., Dolly, J. O. & Pongs, O. (1994) *Nature (London)* **369,** 289–294.
5. Koch, R. O., Wanner, S. G., Koschak, A., Hanner, M., Schwarzer, C., Kaczorowski, G. J., Slaughter, R. S., Garcia, M. L. & Knaus, H. G. (1997) *J. Biol. Chem.* **272,** 27577–27581.
6. Rhodes, K. J., Strassle, B. W., Monaghan, M. M., Bekele-Arcuri, Z., Matos, M. F. & Trimmer, J. S. (1997) *J. Neurosci.* **17,** 8246–8258.
7. Shamotienko, O. G., Parcej, D. N. & Dolly, J. O. (1997) *Biochemistry* **36,** 8195–8201.
8. Coleman, S. K., Newcombe, J., Pryke, J. & Dolly, J. O. (1999) *J. Neurochem.* **73,** 849–858.
9. Felix, J. P., Bugianesi, R. M., Schmalhofer, W. A., Borris, R., Goetz, M. A., Hensens, O. D., Bao, J. M., Kayser, F., Parsons, W. H., Rupprecht, K., *et al*. (1999) *Biochemistry* **38,** 4922–4930.
10. Shi, G., Nakahira, K., Hammond, S., Rhodes, K. J., Schechter, L. E. & Trimmer, J. S. (1996) *Neuron* **16,** 843–852.
11. Lodish, H. F., Kong, N., Snider, M. & Strous, G. J. (1983) *Nature (London)* **304,** 80–83.
12. Pelham, H. R. (1989) *Annu. Rev. Cell Biol.* **5,** 1–23.
13. Manganas, L. N. & Trimmer, J. S. (2000) *J. Biol. Chem.* **275,** 29685–29693.
14. Rhodes, K. J., Keilbaugh, S. A., Barrezueta, N. X., Lopez, K. L. & Trimmer, J. S. (1995) *J. Neurosci.* **15,** 5360–5371.
15. Bekele-Arcuri, Z., Matos, M. F., Manganas, L., Strassle, B. W., Monaghan, M. M., Rhodes, K. J. & Trimmer, J. S. (1996) *Neuropharmacology* **35,** 851–865.
16. Rhodes, K. J., Monaghan, M. M., Barrezueta, N. X., Nawoschik, S., Bekele-Arcuri, Z., Matos, M. F., Nakahira, K., Schechter, L. E. & Trimmer, J. S. (1996) *J. Neurosci.* **16,** 4846–4860.
17. Tiffany, A. M., Manganas, L. N., Kim, E., Hsueh, Y.-P., Sheng, M. & Trimmer, J. S. (2000) *J. Cell Biol.* **148,** 147–157.
18. Nakahira, K., Shi, G., Rhodes, K. J. & Trimmer, J. S. (1996) *J. Biol. Chem.* **271,** 7084–7089.
19. Shi, G., Kleinklaus, A. K., Marrion, N. V. & Trimmer, J. S. (1994) *J. Biol. Chem.* **269,** 23204–23211.
20. Spencer, R. H., Sokolov, Y., Li, H., Takenaka, B., Milici, A. J., Aiyar, J., Nguyen, A., Park, H., Jap, B. K., Hall, J. E., *et al*. (1997) *J. Biol. Chem.* **272,** 2389–2395.
21. Zhou, Z., Gong, Q., Epstein, M. L. & January, C. T. (1998) *J. Biol. Chem.* **273,** 21061–21066.
22. Banker, G. A. & Cowan, W. M. (1977) *Brain Res.* **126,** 397–425.
23. Murakoshi, H. & Trimmer, J. S. (1999) *J. Neurosci.* **19,** 1728–1735.
24. Lim, S. T., Antonucci, D. E., Scannevin, R. H. & Trimmer, J. S. (2000) *Neuron* **25,** 385–397.
25. Chandy, K. G. & Gutman, G. A. (1995) in *Ligand- and Voltage-Gated Ion Channels*, ed. North, R. A. (CRC, Boca Raton, FL), pp. 1–71.
26. Johnston, J. A., Ward, C. L. & Kopito, R. R. (1998) *J. Cell Biol.* **143,** 1883–1898.
27. Marquardt, T. & Helenius, A. (1992) *J. Cell Biol.* **117,** 505–513.
28. Hille, B., Armstrong, C. M. & MacKinnon, R. (1999) *Nat. Med.* **5,** 1105–1109.
29. Li, D., Takimoto, K. & Levitan, E. S. (2000) *J. Biol. Chem.* **275,** 11597–11602.
30. Hopkins, W. F., Demas, V. & Tempel, B. L. (1994) *J. Neurosci.* **14,** 1385–1393.
31. Papazian, D. M. (1999) *Neuron* **23,** 7–10.
32. Levitan, E. S. & Takimoto, K. (2000) *Trends Cardiovasc. Med.* **10,** 317–320.
33. Green, W. N. (1999) *J. Gen. Physiol.* **113,** 163–170.
34. Kopito, R. R. (1999) *Physiol. Rev.* **79,** 167–173.
35. Doyle, D. A., Morais Cabral, J., Pfuetzner, R. A., Kuo, A., Gulbis, J. M., Cohen, S. L., Chait, B. T. & MacKinnon, R. (1998) *Science* **280,** 69–77.
36. Hurst, R. S., Busch, A. E., Kavanaugh, M. P., Osborne, P. B., North, R. A. & Adelman, J. P. (1991) *Mol. Pharmacol.* **40,** 572–576.
37. Imredy, J. P. & MacKinnon, R. (2000) *J. Mol. Biol.* **296,** 1283–1294.
38. MacKinnon, R., Cohen, S. L., Kuo, A., Lee, A. & Chait, B. T. (1998) *Science* **280,** 106–109.